

Supersymmetric Relations Among Electromagnetic Dipole Operators

Michael Graesser^a and Scott Thomas^b

^a*Department of Physics
University of California, Santa Cruz, CA 95064*

^b*Department of Physics
Stanford University, Stanford, CA 94305*

Abstract

Supersymmetric contributions to all leptonic electromagnetic dipole operators have essentially identical diagrammatic structure. With approximate slepton universality this allows the muon anomalous magnetic moment to be related to the electron electric dipole moment in terms of supersymmetric phases, and to radiative flavor changing lepton decays in terms of small violations of slepton universality. If the current discrepancy between the measured and Standard Model values of the muon anomalous magnetic moment is due to supersymmetry, the current bound on the electron electric dipole moment then implies that the phase of the electric dipole operator is less than 2×10^{-3} . Likewise the current bound on $\mu \rightarrow e\gamma$ decay implies that the fractional selectron–smuon mixing in the left–left mass squared matrix, $\delta m_{\mu\bar{e}}^2/m_{\bar{\ell}}^2$, is less than 10^{-4} . These relations and constraints are fairly insensitive to details of the superpartner spectrum for moderate to large $\tan\beta$.

High precision measurements of low energy processes can often provide useful probes of physics beyond the Standard Model. Many processes of this type involve the coupling of a photon to Standard Model fermions, such as anomalous magnetic dipole moments [1], electric dipole moments (EDMs) [2], and rare radiative decays [3]. The effective operators which describe these interactions are all of the electromagnetic dipole form. The magnitude of these operators in general depends on the overall scale and details of the heavy particle mass spectrum as well as the interactions which violate the requisite symmetries.

In supersymmetric theories the one-loop contributions to all the electromagnetic dipole operators have very similar diagrammatic structure. In this paper we point out that in the lepton sector this similarity allows the muon anomalous magnetic moment to be related to the electron EDM in terms of the phase of the electromagnetic dipole operator, and to the rate for radiative lepton decays, $\mu \rightarrow e\gamma$, $\tau \rightarrow \mu\gamma$ and $\tau \rightarrow e\gamma$, in terms of violations of slepton universality. For moderate to large $\tan\beta$ and with approximate slepton universality these relations turn out to be fairly insensitive to details of the superpartner mass spectrum. If the discrepancy between the current measured value of the muon anomalous magnetic moment [4] and the Standard Model value is interpreted as arising from supersymmetry, fairly model independent bounds can be obtained on the phase of the dipole operator and fractional flavor violating splitting in the slepton mass squared matrix from the current experimental bounds on the electron EDM and $\ell_i \rightarrow \ell_j\gamma$ decays respectively. Alternately, an upper limit on the supersymmetric contribution to the muon anomalous magnetic moment provides a lower limit for the most stringent possible bounds arising from the electron EDM and $\ell_i \rightarrow \ell_j\gamma$ decays. The relations among the supersymmetric electromagnetic dipole operators presented here are particularly interesting and useful in light of the recent high precision measurement of the muon anomalous magnetic moment [4]. The relation between the muon anomalous magnetic moment and radiative flavor changing lepton decays has previously been considered in the context of supersymmetric see-saw models of neutrino masses [5].

In the next section the structure of the various supersymmetric contribu-

tions to electromagnetic dipole operators are illustrated. The relative importance of various classes of diagrams are presented and the dominant contribution identified. Under the assumption of slepton universality and proportionality the lepton dipole operators for different generations are shown to be related by ratios of the lepton masses. The manner in which these ratios may be modified by slepton sflavor violation is also described. In section 2 supersymmetric contributions to the muon anomalous magnetic moment are discussed, and the magnitude of possible contributions from sflavor violation evaluated. These contributions are shown generally to be smaller than the flavor conserving contributions. The relationship between the electron EDM and muon anomalous magnetic moment is discussed in section 3. For moderate to large $\tan\beta$ it is shown that the electron EDM is dominated by a single supersymmetric phase to lowest order in gaugino–Higgsino mixing and assuming strict gaugino unification. Under the assumption of slepton universality and proportionality, the most stringent possible model independent limit on this phase arising from the ^{205}Tl EDM experiment consistent with the Brookhaven muon $g-2$ experiment is derived. Contributions to the electron EDM from sflavor violation are also considered, and in particular, important contributions from staus are identified. Radiative flavor changing lepton decays arising from transition dipole moments are considered in section 4. Fairly model-independent stringent bounds on sflavor violating mass squared mixings implied by current limits on $\ell_i \rightarrow \ell_j \gamma$ and consistent with the Brookhaven muon $g-2$ experiment are derived. The manner in which they are model-independent are described below. The complete expressions for the one-loop supersymmetric contributions to electromagnetic dipole operators in the large $\tan\beta$ limit and to first order in gaugino–Higgsino mixing are given in the appendix.

1 Electromagnetic Dipole Operators

The coupling of an on-shell Dirac fermion to the electromagnetic field strength may be represented by the Lagrangian dipole operator

$$-\frac{1}{2}\mathcal{D}_f \bar{f}_L \sigma^{\mu\nu} f_R F_{\mu\nu} - \frac{1}{2}\mathcal{D}_f^* \bar{f}_R \sigma^{\mu\nu} f_L F_{\mu\nu} \quad (1)$$

where \mathcal{D}_f is the dipole moment coefficient, and $f_{L,R} = P_{L,R}f$ are the left- and right-handed chiral components of the Dirac fermion. The dipole moment coefficient can in general be complex and have non-trivial flavor structure. The on-shell dipole operator is chirality violating and so must vanish with the fermion mass. Supersymmetric contributions are therefore proportional to the fermion mass, and suppressed by two powers of the superpartner mass scale, rendering the dipole operator effectively dimension six.

Supersymmetric contributions to anomalous magnetic moments require only violation of chiral symmetry, which is already violated in the Standard Model by the fermion Yukawa couplings. In contrast, electric dipole moments require in addition the violation of parity and time-reversal symmetries beyond that of the Standard Model. And flavor changing radiative decays require violation of flavor symmetries, which in the leptonic sector are not violated within the Standard Model. The strategy here is therefore to use the similarity of the one-loop supersymmetric contributions discussed below to determine the overall scale of the dipole operators from anomalous magnetic moments and to relate this to electric dipole moments in terms of supersymmetric phases which violate parity and time reversal, and to radiative flavor changing decays in terms of supersymmetric violations of flavor symmetries. Experimentally, only the muon anomalous magnetic moment is measured sufficiently accurately to allow the possibility of discerning the supersymmetric contribution. As a practical matter, model independent relations among the dipole operators are therefore only useful in the leptonic sector. Under the mild assumptions of approximate universality and proportionality discussed below, these relations turn out to be rather insensitive to details of the superpartner mass spectrum.

In order to determine the dominant diagrams and relations among the

dipole operators it is instructive to consider the parametric dependences of various contributions. The supersymmetric one-loop contributions to the electromagnetic dipole operators arise from virtual sleptons and charginos or neutralinos. These can be classified according to whether the one-particle-irreducible diagrams are chirality conserving or violating. The chirality conserving diagrams give dimension six operators which reduce to the chirality violating dipole operator (1) on-shell through the external equations of motion. The chirality violating diagrams give the effective dimension six dipole operator (1) directly.

The chargino and neutralino mass eigenstates are general mixtures of the Bino, Wino, and Higgsino interaction eigenstates. However, for $m_i^2 - \mu^2 \gg m_Z^2$, which holds over much of the parameter space, the mixing may be treated perturbatively in $m_Z^2/(m_i^2 - \mu^2)$, where $m_i = \{m_{\tilde{B}}, m_{\tilde{W}}\}$ are the Bino and Wino Majorana mass parameters and μ is the Higgsino Dirac mass parameter. It is therefore sufficient to work to lowest non-trivial order in gaugino-Higgsino mixing. It is seen below that diagrams with gaugino-Higgsino mixing can provide the most important contributions to the dipole moments. In addition, for lepton dipole operators it is sufficient to work to first order in the small lepton Yukawa coupling. This greatly simplifies classification of the supersymmetric diagrams.

The chirality conserving one-loop diagrams for leptons are shown in Fig. 1. Since the use of the external lepton equation of motion to obtain the dipole operator (1) involves the lepton Yukawa coupling it is sufficient consider diagrams which do not include additional powers of the lepton Yukawa. Left-right slepton mixing must vanish with the lepton mass, and so can be ignored in the chirality conserving diagrams. Likewise, the charginos and neutralinos only couple through gaugino components to lowest order since the Higgsino components couple through the lepton Yukawa. The chargino propagator is therefore given by $\langle \tilde{W}^+ \tilde{W}^- \rangle$ where throughout a sum over mass eigenstates is understood. Charginos only contribute to the left-left diagram. For the neutralino diagrams Bino-Wino mixing arises only at second order in gaugino-Higgsino mixing and so the chirality conserving neutralino propagators are given predominantly by $\langle \tilde{W}^{0*} \tilde{W}^0 \rangle$ and $\langle \tilde{B}^* \tilde{B} \rangle$ which contribute

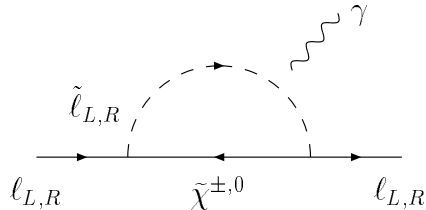


Figure 1: Chirality conserving left–left or right–right contributions to lepton electromagnetic dipole operators. Arrows indicate the flow of fermion or scalar-partner chirality. To lowest order in the fermion Yukawa coupling only gaugino–gaugino propagators contribute to the internal chargino or neutralino propagators. The external photon is attached to internal charged lines in all possible ways.

to the left–left and right–right diagrams respectively. The parametric dependence of the chirality conserving contributions arising from the diagrams of Fig. 1 are

$$\chi \text{ Conserving } RR \langle \tilde{B}^* \tilde{B} \rangle : \mathcal{D}_f \sim \frac{g_1^2 m_\ell}{16\pi^2 \tilde{m}^2} \quad (2)$$

$$\chi \text{ Conserving } LL \langle \tilde{W}^{+,0*} \tilde{W}^{-,0} \rangle : \mathcal{D}_f \sim \frac{g_2^2 m_\ell}{16\pi^2 \tilde{m}^2} \quad (3)$$

where $16\pi^2$ represents the loop factor, \tilde{m} represents the superpartner mass scale determined by the heaviest particle in the loop, and the lepton mass m_ℓ arises from lepton equation of motion. The Bino contributions are suppressed by a factor $g_1^2/g_2^2 = \tan^2 \theta_w$ compared with Wino. The dominant chirality conserving contribution then arises for the left–left diagram through Wino propagators.

The chirality violating one–loop diagrams for leptons are shown in Fig. 2. These diagrams contribute directly to the operator (1) and have an explicit factor of the lepton Yukawa coupling. In the first class of diagrams the lepton Yukawa coupling, λ_ℓ , arises directly in the vertex which couples the down-type Higgsino components of the chargino or neutralino to the slepton and external lepton. To lowest order in the lepton Yukawa the other

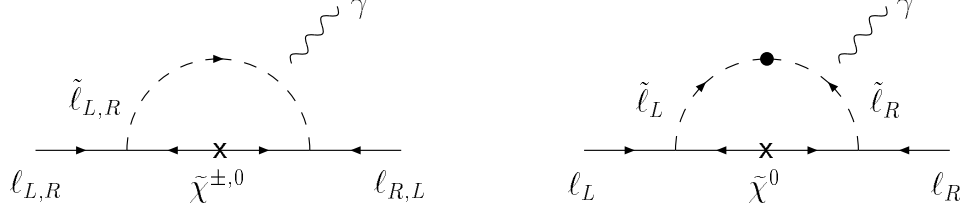


Figure 2: Chirality violating left–right contributions to lepton electromagnetic dipole operators. Arrows indicate the flow of fermion or scalar-partner chirality. A cross indicates a chirality violating propagator. A dot indicates a left–right slepton propagator or equivalently a left–right mass squared mixing chiral insertion. To lowest order in the fermion Yukawa coupling only gaugino–Higgsino propagators contribute to the diagram without a chiral insertion on the scalar line, and only gaugino–gaugino propagators to the diagram with a chiral insertion on the scalar line. The later are dominated by Bino–Bino propagators up to second order in gaugino-Higgsino mixing. The external photon is attached to internal charged lines in all possible ways.

vertex then couples to the gaugino component of the chargino or neutralino proportional to a gauge coupling. Left–right slepton mixing can also be neglected in these diagrams to lowest order in the lepton Yukawa. The chargino propagator in these diagrams is then $\langle \widetilde{W}^+ \widetilde{H}_d^- \rangle$. Since the Wino couples to left-handed fields, only the left handed slepton arises in this class of chargino diagrams. The neutralino propagators are $\langle \widetilde{W}^0 \widetilde{H}_d^0 \rangle$ which arises only with the left-handed slepton and $\langle \widetilde{B} \widetilde{H}_d^0 \rangle$ which arises only with the right-handed slepton. All these propagators require gaugino–Higgsino mixing which arises through coupling with the Higgs condensate proportional to a gauge coupling. To lowest order in mixing the $\langle \widetilde{W}^+ \widetilde{H}_d^- \rangle$ and $\langle \widetilde{W}^0 \widetilde{H}_d^0 \rangle$ chirality violating propagators are proportional to $m_{\widetilde{W}}(g_2 v_u)\mu$ through mixing of chirality violating Wino and Higgsino propagators through the up-type Higgs condensate, and $g_2 v_d$ through mixing of chirality conserving propagators through the down-type Higgs condensate. The chirality violating $\langle \widetilde{B} \widetilde{H}_d^0 \rangle$ propagator is likewise proportional to $m_{\widetilde{B}}(g_1 v_u)\mu$ and $g_1 v_d$. Mixings through the down-type Higgs

condensates are suppressed for moderate to large $\tan\beta = v_u/v_d$. The parametric dependence of this class of chirality violating contributions coming from the first diagram of Fig. 2 in this case are

$$\chi \text{ Violating } LR \langle \widetilde{B}\widetilde{H}_d^0 \rangle : \quad \mathcal{D}_f \sim \frac{g_1^2 m_{\widetilde{B}} \mu m_\ell \tan\beta}{16\pi^2 \widetilde{m}^4} \quad (4)$$

$$\chi \text{ Violating } LR \langle \widetilde{W}^{+,0}\widetilde{H}_d^{-,0} \rangle : \quad \mathcal{D}_f \sim \frac{g_2^2 m_{\widetilde{W}} \mu m_\ell \tan\beta}{16\pi^2 \widetilde{m}^4} \quad (5)$$

where $m_\ell \sim \lambda_\ell v_d$. Even though these contributions require gaugino–Higgsino mixing, they are parametrically enhanced by a factor of $\tan\beta$ with respect to the chirality conserving contributions (2) and (3) because of the coupling to the up-type Higgs condensate.

The second class of chirality violating diagrams involve the lepton Yukawa coupling through left–right scalar mixing. To first order in the lepton Yukawa this mixing may be treated as a mass squared insertion on the slepton propagator. Under the assumption of proportionality of the scalar tri-linear soft A -terms, the left–right mixing mass squared for sleptons is given by $(A - \mu \tan\beta)m_\ell$. The factor of $\mu \tan\beta$ arises from a superpotential cross term between the Higgsino mass parameter and lepton Yukawa coupling which mixes the scalar sleptons through the up-type Higgs condensate. Left–right mixing only occurs for charged sleptons. So only neutralinos contribute to the diagrams with external charged leptons. To lowest order in the lepton Yukawa only the gaugino components of the neutralinos couple the sleptons to the external leptons proportional to a gauge coupling. Only the Bino component of the neutralinos couples to the right-handed slepton. And since $\langle \widetilde{W}^0 \widetilde{B} \rangle$ arises only at second order in gaugino–Higgsino mixing the chirality violating neutralino propagators are given predominantly by $\langle \widetilde{B} \widetilde{B} \rangle$. For moderate to large $\tan\beta$ the parametric dependence of this class of chirality violating contributions coming from the second diagram of Fig. 2 is

$$\chi \text{ Violating } LR \langle \widetilde{B} \widetilde{B} \rangle : \quad \mathcal{D}_f \sim \frac{g_1^2 m_{\widetilde{B}} \mu m_\ell \tan\beta}{16\pi^2 \widetilde{m}^4} \quad (6)$$

where $m_{\widetilde{B}}$ arises from the chirality violating Bino propagator and $\mu \tan\beta$ from left–right slepton mixing. These contributions are also enhanced by a

factor of $\tan \beta$ with respect to the chirality conserving contributions (2) and (3).

For moderate to large $\tan \beta$ the chirality violating contributions to dipole operators should dominate over the chirality conserving ones because of the coupling to the up-type Higgs condensate. Among these, the neutralino contributions (4) and (6) which involve Bino coupling(s) are suppressed by a factor $(g_1^2/g_2^2)m_{\tilde{B}}/m_{\tilde{W}}$ compared with the chargino and neutralino contributions (5) which involve Wino couplings. With gaugino unification $m_{\tilde{B}}/m_{\tilde{W}} \simeq g_1^2/g_2^2$ which implies an overall suppression of $(g_1^4/g_2^4) = \tan^4 \theta_w$. So with slepton universality and proportionality the first diagram of Fig. 2, which includes a left-handed slepton and Wino coupling, should give the dominant contributions to the dipole operator for moderate to large $\tan \beta$ [6, 7]. This expectation is useful in identifying the microscopic phase bounded by the electron EDM discussed in section 3, and the source of slepton flavor violation bounded by $\ell_i \rightarrow \ell_j \gamma$ decays discussed in section 4.

Even though the neutralino and chargino diagrams of the dominant chirality violating contribution are parametrically identical, the loop integrals differ because the external photon does not couple to the same internal lines. For equal superpartner masses the neutralino diagram turns out to be a factor 6 smaller than the chargino [6]. For general superpartner masses the relative importance of these two diagrams depends on the ratios $x \equiv \mu^2/m_{\tilde{W}}^2$ and $y \equiv m_{\tilde{e}_L}^2/m_{\tilde{W}}^2$. An explicit evaluation of these diagrams (see the appendix for details) indicates that the relative importance of the chargino to neutralino diagram strictly increases for large left-handed slepton masses, *i.e.*, for $y > 1, x = 1$, or for small μ , *i.e.*, for $y = 1, x < 1$, and strictly decreases in the other directions in parameter space, that is for small left-handed slepton masses, *i.e.*, for $y < 1, x = 1$, or large μ , *i.e.*, for $y = 1, x > 1$. Even though the ratio is decreasing for $y < 1, x = 1$, the chargino diagram is more important for well-motivated values for y . For example, with $y = 1/10$ the chargino diagram is three times larger than the neutralino diagram, and for the extreme value of $y = 1/100$ it is still twice as large. There is a similar behavior for $y = 1$ with x variable. As noted above, for $x < 1$ the chargino diagram is even more important than for the case of equal superpartner masses. For

$x > 1$ the ratio decreases rather slowly, with the chargino diagram still four times as large even at the extreme value of $x = 100$. We therefore conclude that the chargino first diagram of Fig. 2 is dominant over the neutralino first diagram over essentially all of parameter space.

The importance of the second neutralino diagram of Fig. 2 depends on the size of the μ parameter and the right-handed slepton mass compared to the other superpartner masses. For equal superpartner masses is a factor of $3g_2^2/g_1^2 = 3/\tan^2\theta \simeq 10$ smaller than the dominant chargino diagram discussed above. However, in the limit in which the μ term is much larger than all the other superpartner masses this diagram is easily seen to be larger than the other gaugino-Higgsino diagrams. The reason is that the neutralino diagram with the left-right mass insertion is directly proportional to μ , whereas the diagrams with gaugino-Higgsino propagators decouple at least as fast as μ^{-1} . This behavior is preserved even if the left-handed slepton and Wino masses are large and comparable to μ , whereas the right-handed slepton and Bino masses remain small. In this case the chargino diagram decouples as

$$\mathcal{D}_\mu^{\chi^+} \rightarrow -\frac{eg_2^2}{64\pi^2} \frac{m_\mu^2}{m_L^2} \tan\beta, \quad (7)$$

whereas in the same limit the neutralino second diagram of Fig. 2 with the left-right mass squared insertion decouples more slowly,

$$\mathcal{D}_\mu^{\chi_{LR}^0} \rightarrow -\frac{eg_1^2}{96\pi^2} \frac{m_\mu^2 \mu m_{\tilde{B}}}{m_L^2 m_R^2} \tan\beta \quad (8)$$

and for $\mu \simeq m_{\tilde{e}_L}$ this can easily dominate. As μ is decreased further the chargino diagram becomes dominant. For μ small compared to the Wino and left-handed slepton mass the chargino diagram decouples as m_L^{-3} , but the loop integral has a logarithmic infra-red divergence that is cutoff by μ . In this limit the chargino diagram is

$$\mathcal{D}_\mu^{\chi^+} \rightarrow -\frac{eg_2^2}{16\pi^2} \frac{m_\mu^2 \mu}{m_L^3} \left(\ln\left(\frac{m_L^2}{\mu^2}\right) - \frac{11}{6} \right) \tan\beta \quad (9)$$

whereas the neutralino diagram with the left-right mass insertion is unchanged from (8). In this limit the logarithm is large, and the chargino

diagram still dominates this neutralino diagram for left-handed slepton and wino masses more than roughly 10 times larger than the μ term, Bino, and right-handed slepton masses.

Finally, the importance of the first neutralino diagram of Fig. 2 with Bino coupling and right-handed sleptons, rather than Wino coupling and left-handed sleptons considered above, obviously depends on μ and the right-handed and Bino mass spectrum. If gaugino unification is assumed, $m_{\tilde{B}}/m_{\tilde{W}} = g_1^2/g_2^2$, then this neutralino diagram and the chargino diagram depend on the mass ratios $x \equiv \mu^2/m_{\tilde{W}}^2$, $y \equiv m_{\tilde{e}_L}^2/m_{\tilde{W}}^2$, and $z \equiv m_{\tilde{e}_R}^2/m_{\tilde{W}}^2$. The relative importance of these two diagrams is determined by these ratios. Consider the case with $m_{\tilde{e}_L} = m_{\tilde{W}}$, *i.e.*, $y = 1$. For comparable right-handed and left-handed slepton masses the chargino diagram is dominant. For example, for $z = 1$ corresponding to $m_{\tilde{e}_R} = m_{\tilde{W}}$, the bino neutralino diagram is typically a factor of roughly 10 smaller than the dominant chargino diagram for μ in the range $1/9 < x < 9$. For a right-handed slepton mass small compared to the Wino mass the neutralino diagram may however be comparable to the chargino diagram. More concretely, for $z = 1/9$ corresponding to $m_{\tilde{e}_R} \simeq m_{\tilde{B}} = m_{\tilde{e}_L}/3$, the neutralino diagram is typically less than but comparable to the chargino diagram for various values of μ or x ; the neutralino to chargino diagram ratio for $x = 1/9$ is 0.7, and steadily decreases to 0.5 for $x = 9$.

For even lighter right-handed slepton masses this neutralino diagram remains larger than the chargino diagram by a factor of a few. It might be imagined that in this limit the neutralino diagram scales as an inverse power of the right-handed slepton mass and then easily dominates. In fact, there is no infra-red divergence. This is apparent in the effective theory below the Bino and Higgsino masses. At this scale integrating out the Bino and Higgsino generates a dimension five operator which couples two fermions and two sleptons. This operator contributes at one-loop to the muon dipole operator, and by inspection naively vanishes as the right-handed slepton mass goes to zero. The loop integral however is linearly divergent and this cancels the vanishing mass dependence to leave a finite part. In this limit the Bino

neutralino first diagram of Fig. 2 approaches

$$\mathcal{D}_\mu^{\chi_R^0} \rightarrow \frac{eg_1^2}{32\pi^2} \frac{m_\mu}{\mu m_{\tilde{B}}}. \quad (10)$$

in this limit. Thus the heavier Bino and Higgsino masses set the scale for this contribution rather than the lighter right-handed slepton mass. Comparing this result to the chargino diagram assuming gaugino unification and equal μ term Higgsino mass, Wino mass, and left-handed slepton mass shows that in these limits it is larger by a factor of two than the chargino diagram.

The result is that within the gaugino mass unification assumption the first Bino neutralino diagram of Fig. 2 with right-handed sleptons is actually more important than the chargino diagram for a right-handed slepton mass roughly three times smaller than the mass scale of the $SU(2)_L$ superpartner masses. For heavier right-handed slepton masses the chargino diagram is dominant. Finally, it is interesting to note that for equal superpartner masses and assuming slepton proportionality there is an accidental cancellation between the leading $\tan\beta$ contributions to the Bino neutralino first diagram of Fig. 2 and the second Bino neutralino diagram of Fig. 2 which involves a left–right mass squared insertion.

Independent of which diagrams dominate, up to very small corrections proportional to powers of the lepton Yukawa coupling, all contributions to the lepton dipole operators are proportional to a single power of the lepton mass, as discussed above. With slepton universality and proportionality of the scalar tri-linear soft terms this implies that the dipole operators for different leptons are related simply by ratios of the Yukawa couplings or equivalently lepton masses. This applies diagram by diagram. For example, for the electron and muon

$$\mathcal{D}_e \simeq \frac{m_e}{m_\mu} \mathcal{D}_\mu \quad (11)$$

for both the real and imaginary parts, and likewise for the tau dipole operator. This relation is good over all of parameter space with slepton universality and proportionality. This relation will be used in subsequent sections to relate the muon anomalous magnetic moment to the electron EDM in terms of

the phase of the operator, and to radiative $\ell_i \rightarrow \ell_j \gamma$ decays in terms of small violations of slepton flavor.

Violations of slepton universality and proportionality can in principle modify the relation (11). The magnitude of the scalar tri-linear A -terms for the first two generations are in principle limited only by the requirement that the radiatively induced contribution to the lepton mass not be larger than the observed lepton masses [8]. For non-proportional $A \gtrsim \mu \tan \beta$ the relation (11) would be modified. However, in almost all theories of supersymmetry breaking in which the lepton masses arise in a conventional fashion from tree-level superpotential Yukawa couplings, the A -terms are at most of order of the other supersymmetry breaking mass parameters. Splittings of the \tilde{e} , $\tilde{\mu}$, and $\tilde{\tau}$ masses would also of course modify the precise relation (11). Such splittings depend on the underlying theory of flavor and supersymmetry breaking and in most models are small at least for the first two generations.

More interesting modifications of the relation (11) can arise from sflavor violation in the slepton soft mass squared matrix. For the first two generations, sflavor violating mixings can introduce dependence on a heavier lepton mass. This occurs in the second chirality violating diagrams of Fig. 2. Sflavor violation in the slepton propagators allows left–right mass squared insertions proportional to m_μ or m_τ for the electron dipole operator, and m_τ for the muon. For moderate to large $\tan \beta$ the parametric dependence of this class of chirality violating contributions to the electron and muon dipole operators is

$$\mathcal{D}_e \sim \frac{g_1^2 m_{\tilde{B}} \mu}{16\pi^2 \tilde{m}^4} \left[(\delta_{12}^\ell)_{LL} (\delta_{21}^\ell)_{RR} m_\mu + (\delta_{13}^\ell)_{LL} (\delta_{31}^\ell)_{RR} m_\tau \right] \tan \beta \quad (12)$$

$$\mathcal{D}_\mu \sim \frac{g_1^2 m_{\tilde{B}} \mu}{16\pi^2 \tilde{m}^4} \left[(\delta_{23}^\ell)_{LL} (\delta_{32}^\ell)_{RR} m_\tau \right] \tan \beta \quad (13)$$

where throughout

$$(\delta_{ij}^\ell)_{LL} \equiv \frac{\delta m_{\tilde{\ell}_i L \tilde{\ell}_j L}^2}{m_{\tilde{\ell}_L}^2} \quad (14)$$

represents insertions of sflavor violating left–left mass squared mixings in the slepton propagators, and likewise for right–right and left–right sflavor

violating mass squared terms. The potential importance of these sflavor violating mixing effects in introducing dependence on heavier fermion masses depends on the magnitude of the sflavor violation and on the specific dipole operator. Possible contributions associated to the EDM and flavor changing operators are presented in subsequent sections.

2 Muon Anomalous Magnetic Moment

The anomalous magnetic moment $a_f \equiv (g-2)/2$ of a Dirac fermion is related to the dipole operator (1) by

$$a_f = \frac{2|m_f|}{eQ_f} |\mathcal{D}_f| \cos \varphi \quad (15)$$

where Q_f the fermion electric charge,¹ and in a general basis

$$\varphi \equiv \text{Arg}(\mathcal{D}_f m_f^*) \quad (16)$$

is the relative phase between the dipole operator and fermion mass.

Supersymmetric contributions to the anomalous magnetic dipole moments of various fermions can be related in terms of the microscopic parameters of the theory. As discussed in section 1, slepton universality and proportionality imply that the lepton dipole moment operators are related by ratios of lepton masses (11). With the definition (15) this gives the well known relation that supersymmetric contributions to anomalous magnetic moments are related by ratios of fermion masses squared. For example, for the electron and muon

$$a_e^{\text{SUSY}} \simeq \frac{m_e^2}{m_\mu^2} a_\mu^{\text{SUSY}} \quad (17)$$

and likewise for the tau.

The best measured anomalous magnetic moment in proportion to the fermion mass squared is for the muon. Bounds on, or measurements of, a_μ

¹The electron electric charge is $Q_e = -1$.

therefore provide the most useful information about the overall magnitude of supersymmetric contributions to lepton dipole operators. The Brookhaven muon $g - 2$ experiment has observed a value which differs by at the 2.6σ level from the Standard Model prediction $a_\mu^{\text{exp}} - a_\mu^{\text{SM}} = 43 \pm 16 \times 10^{-10}$ [4]. Additional data and a run utilizing anti-muons will reduce both statistical and systematic errors. The largest theoretical uncertainty in the Standard Model prediction arises from hadronic contributions to photon vacuum polarization. At present there is not a complete concordance among the various theoretical calculations used to extract the photon polarization from $e^+e^- \rightarrow$ hadrons and tau decays. It is of course very important that this uncertainty be better understood [9, 10].

One possible explanation for the experimental discrepancy [4] is the existence of additional non-Standard Model contributions to the muon anomalous magnetic moment. Electroweak scale supersymmetry can easily give contributions to a_μ of the requisite magnitude [11]. The dominant chargino–sneutrino diagram gives a contribution to the muon anomalous magnetic moment of

$$a_\mu^{\chi^\pm} \simeq \frac{g_2^2 \tan \beta m_\mu^2}{32\pi^2 \widetilde{m}^2} \text{sgn}(\mu) \quad (18)$$

where \widetilde{m} is the effective mass of the virtual superpartners. This supersymmetric contribution can account for the discrepancy with $\widetilde{m} \sim 50\sqrt{\tan \beta}$ GeV and $\text{sgn}(\mu) = +$. The total supersymmetric contribution of course depends on details of the superpartner mass spectrum and couplings and is model dependent. However, as detailed in the next two sections, the relation among supersymmetric contributions to electromagnetic dipole operators in terms of violations of time reversal and parity or sflavor symmetries is not particularly sensitive to details of the superpartner spectrum and is fairly model independent. The discrepancy, $a_\mu^{\text{exp}} - a_\mu^{\text{SM}}$, if interpreted as arising from supersymmetry, may therefore be used to set the overall scale for supersymmetric contributions to all lepton electromagnetic dipole operators. Alternately, the discrepancy may be interpreted as an upper limit on the overall scale of supersymmetric contributions to lepton dipole operators.

The muon anomalous magnetic moment, or equivalently the dipole moment coefficient, may be used to set the scale for other lepton dipole operators

through the relations (11) and (17). Since these relations assume slepton universality and proportionality it is important to consider the magnitude of possible modifications of these relations from violations of universality or proportionality. As mentioned at the end of section 1, dependence of a dipole operator on a heavier lepton mass can be introduced by slepton flavor violation. For the muon dipole operator the presence of both right–right and left–left smuon–stau mixing gives a contribution (13) proportional to m_τ through flavor conserving left–right stau mixing in the chirality violating Bino second diagram of Fig. 2. In terms of insertions this corresponds to smuon–stau mixing insertions on both the left and right handed slepton lines and a left–right stau mixing insertion proportional to m_τ represented by a dot in the second diagram of Fig. 2. For moderate to large $\tan\beta$ the parametric dependence of the sflavor violating contribution (13) arising from stau mixing proportional to m_τ in the Bino diagram, compared to the dominant flavor conserving contribution (5) is

$$\frac{a_\mu^{\text{SUSY}-\tilde{\tau}}}{a_\mu^{\text{SUSY}-\tilde{\mu}}} \simeq \frac{g_1^2}{3g_2^2} \frac{m_\tau}{m_\mu} \frac{m_{\tilde{B}}}{m_{\tilde{W}}} (\delta_{23}^\ell)_{LL} (\delta_{32}^\ell)_{RR} \frac{h_0}{f_+} h_{0,LR}'' \quad (19)$$

where the sflavor violating mixing masses squared are treated as insertions, and here it is understood that the flavor violating insertions refer to the real parts only. The functions f_+ and h_0 are loop functions defined in the appendix for the chargino first diagram of Fig. 2 and the neutralino second diagram of Fig. 2, and normalized to unity for equal superpartner masses. The dimensionless derivative function

$$h_{0,LR}'' \equiv \frac{m_{\tilde{\ell}_L}^2 m_{\tilde{\ell}_R}^2}{h_0} \frac{\partial^2 h_0}{\partial m_{\tilde{\ell}_L}^2 \partial m_{\tilde{\ell}_R}^2} = \frac{1}{h_0} \frac{\partial^2 h_0}{\partial \ln m_{\tilde{\ell}_L}^2 \partial \ln m_{\tilde{\ell}_R}^2} \quad (20)$$

represents the modification of the loop function induced by the two sflavor violating mixing insertions such that $h_0 h_{0,LR}''$ is the loop function for the stau contribution $a_\mu^{\text{SUSY}-\tilde{\tau}}$. This function does not differ significantly from unity and is fairly insensitive to details of the superpartner mass spectrum since it is a logarithmic derivative of the loop function. The ratio of loop functions h_0/f_+ does however depend on the superpartner spectrum. For

equal sparticle masses $h_0/f_+ = 1$ and $h''_{0,LR} = 2/5$. With gaugino unification $m_{\tilde{B}}/m_{\tilde{W}} = g_1^2/g_2^2$, the ratio (19) is then roughly $\mathcal{O}(10^{-1} - 1) \times (\delta_{23}^\ell)_{LL}(\delta_{23}^\ell)_{RR}$. So a significant sflavor violating supersymmetric contribution to the muon anomalous magnetic moment would require essentially maximal smuon–stau mixing in both the left–left and right–right channels.

The magnitude of possible sflavor violating mixings is bounded by radiative flavor changing lepton decays, as discussed in section 4. The bounds depend on the overall magnitude of the electromagnetic dipole operators, which as discussed here may be related to the muon anomalous magnetic moment. First, assume that a_μ^{SUSY} is dominated by the flavor conserving chargino contribution, and that the discrepancy $a_\mu^{\text{exp}} - a_\mu^{\text{SUSY}}$ [4] is interpreted as arising from supersymmetry. In this case limits on $\tau \rightarrow \mu\gamma$ radiative decay discussed in section 4 imply that $(\delta_{23}^\ell)_{LL}(\delta_{32}^\ell)_{RR} \lesssim 10^{-1}$ up to model dependent ratios of loop functions. So possible sflavor violating contributions to a_μ^{SUSY} are subdominant in this case. If supersymmetric contributions to the muon anomalous magnetic moment are in fact smaller than the current discrepancy $a_\mu^{\text{exp}} - a_\mu^{\text{SUSY}}$ then the bound on sflavor violating mixings are weakened since the overall magnitude of all electromagnetic dipole operators is smaller. To estimate the importance of this effect consider the Brookhaven muon $g - 2$ experiment which may reach an ultimate sensitivity of $\Delta a_\mu^{\text{exp}} \sim 4 \times 10^{-10}$ [12]. If agreement with an improved calculation of the Standard Model contribution were obtained at this level then the bound on a_μ^{SUSY} would improve by approximately an order of magnitude. This would weaken the bounds obtained in section 4 derived under the assumption that the sflavor conserving chargino contribution dominates a_μ^{SUSY} to roughly $(\delta_{23}^\ell)_{LL}(\delta_{32}^\ell)_{RR} \lesssim 1$ again up to model dependent ratios of loop functions. In this case the sflavor violating stau–Bino contribution could be at most comparable to the flavor conserving smuon–chargino contribution.

So we conclude that for any value of a_μ^{SUSY} which could be accessible to the ultimate sensitivity of the Brookhaven muon $g - 2$ experiment, sflavor violating stau contributions to a_μ^{SUSY} are at most comparable to the flavor conserving contribution (which would require that both left–left and right–right smuon–stau mixing are near maximal), and in fact are an order of

magnitude smaller if the current discrepancy $a_\mu^{\text{exp}} - a_\mu^{\text{SM}}$ [4] is due to supersymmetry. This allows a_μ^{SUSY} to be identified with the dominant sflavor conserving chargino contribution for moderate to large $\tan\beta$ over most of parameter space. And in turn the overall scale for other electromagnetic dipole operators may then be related to a_μ^{SUSY} through the relations (11) and (15).

3 Electron Electric Dipole Moment

An electric dipole moment (EDM) coupling the spin of a fermion to the electric field is odd under both parity and time-reversal. The dipole operator (1) in general violates both these symmetries and is related to the electric dipole moment by

$$d_f = |\mathcal{D}_f| \sin \varphi \quad (21)$$

where φ is the relative phase (16) between the dipole operator coefficient and fermion mass. An EDM requires that this relative phase be non-vanishing.

Under the assumption of slepton universality and proportionality the electron and muon dipole operator coefficients, including the phase, are related by the ratio of masses (11). The supersymmetric contribution to the electron EDM may then be related to the supersymmetric contributions to the muon anomalous magnetic moment by

$$\begin{aligned} d_e^{\text{SUSY}} &\simeq -e \frac{m_e}{2m_\mu^2} a_\mu^{\text{SUSY}} \tan \varphi \\ &\simeq -4.6 \times 10^{-16} a_\mu^{\text{SUSY}} \tan \varphi \text{ e cm} \end{aligned} \quad (22)$$

This relation is independent of which diagrams dominate the dipole operator, or any details of the superpartner spectrum. It is valid over all of parameter space if slepton universality and proportionality holds.

If the current discrepancy between a_μ^{exp} and a_μ^{SM} [4] is interpreted as arising from supersymmetry, $a_\mu^{\text{SUSY}} \sim 42 \times 10^{-10}$, the current bound on the electron EDM of $|d_e| < 4 \times 10^{-27} \text{ e cm}$ obtained from ^{205}Tl [13] along with the relation (22) can be used to obtain a bound on the phase of supersymmetric contribution to the dipole operator of

$$|\tan \varphi| \lesssim 2 \times 10^{-3}$$

Alternately if $a_\mu^{\text{exp}} - a_\mu^{\text{SM}}$ is taken as an upper limit on a_μ^{SUSY} , the above bound can be interpreted as the most stringent possible bound the ²⁰⁵Tl EDM experiment places on the phase of the dipole operator consistent with the bound on a_μ^{SUSY} .

The relation of the phase of the dipole operator to the underlying phases of the supersymmetric Lagrangian depends in principle on the relative importance of the individual diagrams. As discussed in section 1, for moderate to large $\tan\beta$ the chirality violating diagrams of Fig. 2 are all parametrically larger by a factor of $\tan\beta$ than the chirality conserving diagrams of Fig. 1. In order to relate the phase of the dipole operator in this limit to underlying supersymmetric phases it is instructive to determine the origin of the phase of each chirality violating diagram. All the supersymmetric phases arise from relevant terms in the supersymmetric and supersymmetry breaking Lagrangians, and appear in the neutralino, chargino, and slepton mass matrices and therefore propagators after electroweak symmetry breaking.

Consider first the dominant chargino diagram of Fig. 2. This diagram involves a sneutrino propagator, which with slepton universality does not involve a phase. The chirality violating chargino propagator may be obtained to lowest order in Wino-Higgsino mixing by treating the mixing induced by the Higgs condensate as an insertion. In Weyl notation this propagator is

$$\langle \widetilde{W}^+ \widetilde{H}_d^- \rangle \simeq \frac{i\not{p}(-ig_2 v_d/\sqrt{2})i\not{p} + im_{\widetilde{W}}^*(-ig_2 v_u^*/\sqrt{2})i\mu^*}{(p^2 - |m_{\widetilde{W}}|^2)(p^2 - |\mu|^2)} \quad (23)$$

where $v_{u,d} \equiv \sqrt{2}\langle H_{u,d}^0 \rangle$ are the up- and down-type Higgs boson expectation values. The first term in (23) arises from chirality conserving Wino and Higgsino propagators connected through the mixing insertion to the down-type Higgs condensate, while the second arises from the chirality violating propagators connected through the up-type Higgs condensate. Including the lepton Yukawa, λ_ℓ , from the Higgsino-lepton-slepton coupling, the dipole operator phase arising from the first term in (23) proportional to the down-type Higgs condensate is $\text{Arg}(\mathcal{D}_\ell) = \text{Arg}(\lambda_\ell v_d)$, while that from the second term proportional to the up-type Higgs condensate is $\text{Arg}(\mathcal{D}_\ell) = \text{Arg}(\lambda_\ell m_{\widetilde{W}}^* \mu^* v_u^*)$. The physical phase relevant for the EDM is the relative phase (16) between

the dipole operator and lepton mass $\varphi \equiv \text{Arg}(\mathcal{D}_\ell m_\ell^*)$. The phase of the lepton mass in a general basis is determined by the down-type Higgs boson expectation value $\text{Arg}(m_\ell) = \text{Arg}(\lambda_\ell v_d)$. The physical phase arising from the first term in the propagator (23) therefore vanishes $\text{Arg}(\mathcal{D}_\ell m_\ell^*) = \text{Arg}(\lambda_\ell v_d \lambda_\ell^* v_d^*) = 0$, and so contributes only to the magnetic dipole moment. The magnitude of this contribution is however suppressed with respect to the second term in the propagator for large $\tan \beta$, as discussed in section 1. The physical phase arising from the second term in the propagator (23) along with the lepton Yukawa, λ_ℓ , from the Higgsino–lepton–slepton coupling is $\text{Arg}(\mathcal{D}_\ell m_\ell^*) = \text{Arg}(\lambda_\ell^* m_{\tilde{W}}^* \mu^* v_u^* \lambda_\ell v_d^*) = -\text{Arg}(m_{\tilde{W}} \mu v_u v_d)$. In the ground state with broken electroweak symmetry the relative phase of the up- and down-type Higgs condensates is anti-aligned with the Higgs up–Higgs down soft mass parameter, $\text{Arg}(v_u v_d) = -\text{Arg}(m_{ud}^2)$, where $V \supset m_{ud}^2 H_u H_d + h.c.$ [14]. The phase of the dominant chirality violating chargino–sneutrino contribution to the lepton EDM to lowest order in Wino-Higgsino mixing and to leading order in $(\tan \beta)^{-1}$ is therefore given by the basis independent combination of phases [14]

$$\varphi \simeq -\text{Arg} \left(m_{\tilde{W}} \mu (m_{ud}^*)^2 \right) \quad (24)$$

Next consider the neutralino first diagram of Fig. 2. With slepton universality the slepton propagator does not involve a phase. The chirality violating neutralino propagator diagram receives contributions at lowest order from both Wino-Higgsino and Bino-Higgsino mixing. The $\langle \tilde{W}^0 \tilde{H}_d^0 \rangle$ propagator is identical to the propagator (23) including phases. The physical phase of the leading contribution in $(\tan \beta)^{-1}$ is therefore identical to chargino diagram phase (24). The Bino–Higgsino propagator to lowest order in mixing in Weyl notation is very similar

$$\langle \tilde{B} \tilde{H}_d^0 \rangle \simeq \frac{i \not{p} (-ig_1 v_d / \sqrt{2}) i \not{p} + i m_{\tilde{B}}^* (-ig_1 v_u^* / \sqrt{2}) i \mu^*}{(p^2 - |m_{\tilde{B}}|^2) (p^2 - |\mu|^2)} \quad (25)$$

Applying the same discussion of the relative phases as given above for the chargino diagram then implies that the basis independent physical combination of phases arising at leading order in $(\tan \beta)^{-1}$ from this diagram is

$$\varphi \simeq -\text{Arg} \left(m_{\tilde{B}} \mu (m_{ud}^*)^2 \right) \quad (26)$$

With strict gaugino unification $\text{Arg}(m_{\tilde{B}}) = \text{Arg}(m_{\tilde{W}})$. So in this case the phase of this contribution is also identical that of the chargino diagram (24).

Finally, consider the neutralino second diagram of Fig. 2. The slepton propagator includes left–right mixing which in a general basis can involve a phase. To lowest order the left–right mass squared mixing this may be treated as an insertion in the slepton propagator. With slepton universality and proportionality

$$\langle \tilde{\ell}_L \tilde{\ell}_R^* \rangle \simeq \frac{i [i\lambda_\ell (Av_d - \mu^* v_u^*)] i}{(p^2 - m_{\tilde{\ell}_L}^2)(p^2 - m_{\tilde{\ell}_R}^2)} \quad (27)$$

The first term in the numerator arises from the soft scalar tri-linear A term mixing left- and right-handed sleptons through the down-type Higgs condensate, while the second term arises from a superpotential cross term between the Higgsino mass parameter and lepton Yukawa coupling through the up-type Higgs condensate. Through second order in mixing, the chirality violating neutralino propagator of this diagram is dominated by the Bino component. In Weyl notation this propagator is

$$\langle \tilde{B} \tilde{B} \rangle \simeq \frac{im_{\tilde{B}}^*}{(p^2 - |m_{\tilde{B}}|^2)} \quad (28)$$

The dipole operator phase arising from the first term in slepton propagator (27) proportional to the down-type Higgs condensate along with the phase of the Bino propagator (28) is $\text{Arg}(\mathcal{D}_\ell) = \text{Arg}(\lambda_\ell Av_d m_{\tilde{B}}^*)$. The physical phase $\text{Arg}(\mathcal{D}_\ell m_\ell^*)$ from these terms is therefore given by the basis independent combination of phases [14]

$$\varphi \simeq \text{Arg} \left(Am_{\tilde{B}}^* \right) \quad (29)$$

With slepton proportionality the magnitude of this term is however suppressed with respect to the second term in the slepton propagator for moderate to large $\tan \beta$ since it is proportional to the down-type Higgs condensate. The dipole operator phase arising from the second term in the slepton propagator (27) proportional to the up-type Higgs condensate along with the phase of the Bino propagator (28) is $\text{Arg}(\mathcal{D}_\ell) = \text{Arg}(\lambda_\ell \mu^* v_u^* m_{\tilde{B}}^*)$. Anti-alignment of

the relative phase of the up- and down-type Higgs condensates with the Higgs up–Higgs down soft mass parameter, $\text{Arg}(v_u v_d) = -\text{Arg}(m_{ud}^2)$, then implies that the physical phase $\text{Arg}(\mathcal{D}_\ell m_\ell^*)$ is given by the basis independent combination of phases (24). So under the assumption of slepton universality, proportionality and gaugino unification, *all* the $\tan\beta$ enhanced electromagnetic dipole operator diagrams have the same phase to leading order in Higgsino-gaugino mixing. The phase (24) therefore dominates the phase appearing in the electron EDM for moderate to large $\tan\beta$ over most of parameter space.

It might have been possible in principle for the phases among various contributions to the dipole operator to have accidentally approximately canceled [15]. This could in principle occur for small $\tan\beta$ by a cancelation between the phases (24) and (29). But the Bino diagram proportional to the phase (29) is parametrically suppressed by ratios of gauge couplings compared with the dominant chargino diagram. Cancelation would only occur if the ratio of the phases (24) and (29) just happens to be nearly equal in magnitude and opposite in sign to the ratio of the chargino to Bino contributions. Cancelations might also in principle occur in the region of parameter space with large Higgsino-gaugino mixing. However, such fortuitous cancelations depend on accidental details of the superpartner spectrum, are not enforced by any symmetry, and occur only over very narrow slivers of parameter space [16]. Outside of these narrow regions of parameter space the electron EDM can therefore be considered to bound the phase (24) rather directly for moderate to large $\tan\beta$ under the assumption of slepton universality and proportionality.

Slepton flavor violation can in principle lead to violations of the proportionality relation (11). Left–left and right–right sflavor violation in the slepton propagators allows flavor conserving left–right mass squared insertions proportional to both m_μ and m_τ in the electron electromagnetic dipole operator as illustrated in (12). This sflavor violation can introduce important additional sources for the physical phase appearing in the electron EDM. The intermediate stau contribution to the electron EDM proportional to m_τ through a left–right mixing arises from the second neutralino diagram of Fig. 2 with both left–left and right–right selectron–stau flavor violating mass

squared insertions. The ratio of the stau–Bino contribution to the electron EDM to the flavor conserving contribution from the selectron–chargino first diagram of Fig. 2 is

$$\frac{d_e^{\text{SUSY}-\tilde{\tau}}}{d_e^{\text{SUSY}-\tilde{e}}} \simeq \left(\frac{g_1^2}{3g_2^2} \frac{m_\tau}{m_e} \frac{m_{\tilde{B}}}{m_{\tilde{W}}} \right) |(\delta_{13}^\ell)_{LL}(\delta_{31}^\ell)_{RR}| \frac{h_0}{f_+} h_{0,LR}'' \frac{\sin(\varphi + \varphi_{1331})}{\sin \varphi} \quad (30)$$

where φ is the relative phase between the flavor conserving contribution to the dipole operator and electron mass (16) and

$$\varphi_{1331} = \text{Arg} \left((\delta_{13}^\ell)_{LL}(\delta_{31}^\ell)_{RR} \right) \quad (31)$$

is the phase of the left–left times right–right selectron–stau mass squared mixing, and where strict gaugino unification, $\text{Arg}(m_{\tilde{B}}) = \text{Arg}(m_{\tilde{W}})$, has been assumed. The functions f_+ and h_0 are loop functions defined in the appendix for the chargino first diagram of Fig. 2 and the neutralino second diagram of Fig. 2, and normalized to unity for equal superpartner masses. The dimensionless derivative function $h_{0,LR}''$ defined in (20) represents the modification of the loop function induced by the two sflavor violating mixing insertions such that $h_0 h_{0,LR}''$ is the loop function for the stau contribution $d_e^{\text{SUSY}-\tilde{\tau}}$.

The importance of the sflavor violating stau contribution to the electron EDM depends on the magnitude and phases of the left–left and right–right selectron–stau mass squared mixings. With gaugino unification, the first term in parenthesis on the right hand side of the ratio (30) is $(m_\tau/3m_e) \tan^4 \theta_w \simeq 100$. The most stringent possible limits on the magnitude of left–left and right–right selectron–stau sflavor violation arising from the limits on $\tau \rightarrow e\gamma$ radiative decay, and consistent with the current experimental results for the muon anomalous magnetic moment, are presented in section 4. The bounds derived there imply that at best $|(\delta_{13}^\ell)_{LL}(\delta_{31}^\ell)_{RR}| \lesssim 10^{-1}$ up to ratios of model dependent loop functions. Since the sflavor violating phases are unconstrained, the m_τ enhanced sflavor violating stau contribution to the electron EDM could clearly dominate the flavor conserving contribution. So unlike the muon anomalous magnetic moment discussed in section 2, the electron EDM can potentially receive significant contributions from sflavor violation.

The muon anomalous magnetic moment is likely to be dominated by sflavor conserving contributions for any a_μ^{SUSY} which will be accessible to the ultimate sensitivity of the Brookhaven muon $g - 2$ experiment [12], as discussed in section 2. The sflavor conserving supersymmetric contribution a_μ^{SUSY} may then still be used to characterize the magnitude of the sflavor violating stau contribution to the electron EDM in terms of sflavor violation and ratios of loop functions. From the ratio (30) and the relation between the flavor conserving contribution to the electron EDM and a_μ^{SUSY} given in (22), the sflavor violating stau contribution may be written

$$\begin{aligned}
d_e^{\text{SUSY}-\tilde{\tau}} &\simeq -\frac{g_1^2}{6g_2^2} \frac{m_\tau}{m_\mu^2} \frac{m_{\tilde{B}}}{m_{\tilde{W}}} a_\mu^{\text{SUSY}} |(\delta_{13}^\ell)_{LL}(\delta_{31}^\ell)_{RR}| \frac{h_0}{f_+} h''_{0,LR} \times \\
&\quad (\tan \varphi \cos \varphi_{1331} + \sin \varphi_{1331}) \quad e \text{ cm} \\
&\simeq -4.9 \times 10^{-14} a_\mu^{\text{SUSY}} |(\delta_{13}^\ell)_{LL}(\delta_{31}^\ell)_{RR}| \frac{h_0}{f_+} h''_{0,LR} \times \\
&\quad (\tan \varphi \cos \varphi_{1331} + \sin \varphi_{1331}) \quad e \text{ cm} \tag{32}
\end{aligned}$$

If the current discrepancy between a_μ^{exp} and a_μ^{SM} [4] is interpreted as arising from supersymmetry, $a_\mu^{\text{SUSY}} \sim 42 \times 10^{-10}$, the current bound on the electron EDM of $|d_e| < 4 \times 10^{-27} e \text{ cm}$ obtained from ^{205}Tl [13] along with the relation (32) can be used to obtain a bound on the imaginary part of the product of the left–left times right–right selectron–stau mass squared mixings

$$|(\delta_{13}^\ell)_{LL}(\delta_{31}^\ell)_{RR}| |\sin \varphi_{1331}| \lesssim 2 \times 10^{-5} \left(\frac{h_0}{f_+} h''_{0,LR} \right)^{-1}$$

where possible cancelation with the flavor conserving contribution has been ignored. If the sflavor violating phase are large, the electron EDM apparently provides a more stringent bound on the the product left–left times right–right selectron–stau mixing than that obtained from $\tau \rightarrow e\gamma$ decay discussed in section 4. Alternatively, an observation of $\tau \rightarrow e\gamma$ close to the current experimental limit combined with the electron EDM constraint would yield a very strong direct bound on this product of sflavor violating phases.

The electron EDM can also receive analogous sflavor violating contributions proportional to m_μ through sflavor conserving left–right smuon mixing

in combination with both left–left and right–right selectron–smuon mixing, as illustrated in (12). The ratio of this contribution to the sflavor conserving chargino contribution is identical to (30) with m_τ replaced by m_μ , and stau mixing replaced by smuon mixing. This contribution should be smaller than the possible stau contribution discussed above for two reasons. First, the smuon contribution is proportional to m_μ rather than m_τ . Second, the bounds on selectron–smuon mixing are much more stringent than those on selectron–stau mixing. The most stringent possible limits derived in section 4 on selectron–smuon sflavor violation arising from limits on $\mu \rightarrow e\gamma$ radiative decay, and consistent with the current experimental results for the muon anomalous magnetic moment, imply that at best $|(\delta_{12}^\ell)_{LL}(\delta_{21}^\ell)_{RR}| \lesssim 10^{-7}$ up to ratios of model dependent loop functions. In this case the smuon contribution to the electron EDM is smaller than the sflavor conserving selectron–chargino contribution unless the sflavor conserving phase is smaller than the sflavor violating phase by a factor of roughly 10^{-6} .

4 Radiative Flavor Changing Lepton Decays

Non–trivial flavor structure of the electromagnetic dipole operators gives rise to radiative flavor changing fermion decays. There are two possible chiral structures for such transition dipole moments. For example, for μ – e transitions the operators are

$$-\frac{1}{2}\mathcal{D}_{Le\mu} \bar{e}_L \sigma^{\mu\nu} \mu_R F_{\mu\nu} - \frac{1}{2}\mathcal{D}_{Le\mu}^* \bar{\mu}_R \sigma^{\mu\nu} e_L F_{\mu\nu} \quad (33)$$

$$-\frac{1}{2}\mathcal{D}_{Re\mu} \bar{e}_R \sigma^{\mu\nu} \mu_L F_{\mu\nu} - \frac{1}{2}\mathcal{D}_{Re\mu}^* \bar{\mu}_L \sigma^{\mu\nu} e_R F_{\mu\nu} \quad (34)$$

where the subscript L or R refers to the chirality of the lighter final state fermion, and likewise for τ – μ and τ – e operators. The lepton radiative flavor changing decay rates arising from transition operators of the form (33) and (34) are

$$\Gamma(\ell_i \rightarrow \ell_j \gamma) = \frac{(|\mathcal{D}_{Lij}|^2 + |\mathcal{D}_{Rij}|^2) m_{\ell_i}^3}{16\pi} \quad (35)$$

where the left- and right-handed operators do not interfere up to corrections of order m_j^2/m_i^2 [17].

The supersymmetric Standard Model allows for the possibility of individual lepton flavor violation in the left- and right-handed slepton soft mass squared matrices and in the scalar tri-linear soft A -terms mixing left- and right-handed sleptons. These flavor violations appear in the slepton propagators after electroweak symmetry breaking. The supersymmetric diagrams which contribute to the transition dipole operators are just those of section 1 with the inclusion of slepton flavor violating propagators. If the flavor violation in these propagators is small, it may be represented by left–left, right–right and left–right flavor violating mass squared insertions. In this case the magnitude of the flavor violating operators may be related to that of the flavor conserving operators in terms of the small flavor violation. Under the various assumptions detailed below, the muon anomalous magnetic moment may then be related to the decay rates of radiative flavor changing decays $\ell_i \rightarrow \ell_j \gamma$ in terms of flavor violating mass squared insertions.

Consider first the assumption of approximate slepton universality and approximate proportionality which we define as sflavor violation which is small enough so as not to modify the relation (11) that flavor conserving dipole operators are in proportion to the fermion masses. In this case the leading effects come from single insertions of flavor violating mass squared insertions. Possible modifications of approximate universality and proportionality arising from sflavor violation are considered separately below. As discussed in section 1 the chirality violating chargino–sneutrino first diagram of Fig. 2 generally gives the dominant contribution to the flavor conserving dipole operators for moderate to large $\tan\beta$. In this case, ignoring possible cancellations with sub-dominant diagrams discussed below, the supersymmetric contributions to the transition dipole moment for $\ell_i \rightarrow \ell_j \gamma$ can be related to the flavor conserving muon dipole moment in terms of sneutrino flavor violating left–left mass squared insertions in the chargino-sneutrino diagram as

$$\mathcal{D}_{Lij} \supset \frac{m_i}{m_\mu} \mathcal{D}_\mu (\delta_{ij}^\ell)_{LL} f'_{+,L} \quad (36)$$

where the flavor conserving $\mathcal{D}_i \simeq (m_i/m_\mu) \mathcal{D}_\mu$ is assumed to be dominated by

chargino-sneutrino diagram, and $(\delta_{ij}^\ell)_{LL}$ is the dimensionless sflavor violating left–left mixing defined in terms of the left–left mixing mass squared matrix in (14). The dimensionless derivative function

$$f'_{+,L} \equiv \frac{m_{\tilde{\nu}}^2}{f_+} \frac{\partial f_+}{\partial m_{\tilde{\nu}}^2} = \frac{\partial \ln f_+}{\partial \ln m_{\tilde{\nu}}^2} \quad (37)$$

represents the modification of the loop function induced by the left–left sflavor violating insertion on the sneutrino propagator such that $f_+ f'_{+,L}$ is the loop function for the transition dipole operator with $f_+ = f_+(m_{\tilde{\nu}}^2, m_{\tilde{W}}^2, \mu^2)$ the loop function of the dominant chirality violating chargino first diagram of Fig. 2. This order one function depends on details of the superpartner mass spectrum. For equal superpartner masses $f'_{+,L} = -0.4$, while for $0.1 < m_{\tilde{\nu}}^2/m_{\tilde{W}}^2 < 10$ with $m_{\tilde{W}} = \mu$ it varies in the range $-0.11 < f'_{+,L} < -0.75$. Aside from this slight model dependence from modification of the loop function, the transition dipole moment induced by left–left sflavor violation is related rather directly to the muon dipole moment by (37) for moderate to large $\tan \beta$ and assuming approximate universality.

Transition dipole moments can also receive contributions from left–right and right–right sflavor violation through diagrams which are sub-dominant in the flavor conserving dipole moments. The importance of these diagrams depends on the relative magnitude of the underlying sflavor violations. Left–right sflavor violation contributes to transition dipole operators through the chirality violating neutralino second diagram of Fig. 2. The left–right slepton mixing insertion represented by the dot in the second diagram Fig. 2 in this case is flavor violating. Since this diagram does not involve an explicit Yukawa coupling in the neutralino coupling, it contributes to both chiralities of transition operators (33) and (34)

$$\mathcal{D}_{Lij}, \mathcal{D}_{Rij} \supset \frac{m_i}{m_\mu} \mathcal{D}_\mu \frac{g_1^2}{3g_2^2} \frac{m_{\tilde{B}}}{m_{\tilde{W}}} \frac{h_0}{f_+} \frac{m_{\tilde{\ell}_L} m_{\tilde{\ell}_R}}{m_i \mu \tan \beta} (\delta_{ij}^\ell)_{RL} \quad (38)$$

The factor $(g_1^2 m_{\tilde{B}}/g_2^2 m_{\tilde{W}})(h_0/f_+)$ accounts for the difference in loop function and parametric dependence of the couplings and gaugino mass insertions and of the subdominant neutralino second diagram of Fig. 2 compared with the

dominant chargino first diagram. The loop functions are normalized to unity for equal superpartner masses. The factor $m_{\tilde{\ell}_L} m_{\tilde{\ell}_R} / (m_i \mu \tan \beta)$ accounts for the difference in parametric dependence of the flavor conserving and violating left–right mass squared insertions.

Right–right sflavor violation contributes to transition dipole operators at lowest order through two diagrams. The first is the chirality violating neutralino first diagram of Fig. 2 with a right–right mass squared mixing insertion on the slepton propagator. The second is the chirality violating neutralino second diagram of Fig. 2 with again a right–right mass squared insertion on the right handed slepton propagator. Both these diagrams have the same parametric dependence on couplings and chirality violating mass insertions on the neutralino propagators

$$\mathcal{D}_{Rij} \supset \frac{m_i}{m_\mu} \mathcal{D}_\mu \frac{g_1^2}{3g_2^2} \frac{m_{\tilde{B}}}{m_{\tilde{W}}} \left(\frac{-f_0}{f_+} f'_{0,R} + \frac{h_0}{f_+} h'_{0,R} \right) (\delta_{ij}^\ell)_{RR} \quad (39)$$

where $(\delta_{ij}^\ell)_{RR}$ is the dimensionless slepton sflavor violating right–right mixing.

In order to display the relation between the transition dipole moments, the muon anomalous magnetic moment which determines the overall scale for the dipole moments, and sflavor violating mass squared insertions, it is convenient to define the transition dipole operator coefficients in terms of the scaled flavor conserving dipole operator coefficient times dimensionless flavor violating transition elements

$$\begin{aligned} \mathcal{D}_{Lij} &\simeq -e \frac{m_i}{2m_\mu^2} a_\mu^{\text{SUSY}} \epsilon_{Lij} \\ \mathcal{D}_{Rij} &\simeq -e \frac{m_i}{2m_\mu^2} a_\mu^{\text{SUSY}} \epsilon_{Rij} \end{aligned} \quad (40)$$

The leading sflavor violating contributions discussed above then give

$$\epsilon_{Lij} \simeq (\delta_{ij}^\ell)_{LL} f'_{+,L} + \frac{g_1^2}{3g_2^2} \frac{m_{\tilde{B}}}{m_{\tilde{W}}} \frac{h_0}{f_+} \frac{m_{\tilde{\ell}_L} m_{\tilde{\ell}_R}}{m_i \mu \tan \beta} (\delta_{ij}^\ell)_{RL} \quad (41)$$

$$\epsilon_{Rij} \simeq \frac{g_1^2}{3g_2^2} \frac{m_{\tilde{B}}}{m_{\tilde{W}}} \left[\left(\frac{-f_0}{f_+} f'_{0,R} + \frac{h_0}{f_+} h'_{0,R} \right) (\delta_{ij}^\ell)_{RR} + \frac{h_0}{f_+} \frac{m_{\tilde{\ell}_L} m_{\tilde{\ell}_R}}{m_i \mu \tan \beta} (\delta_{ij}^\ell)_{RL} \right] \quad (42)$$

Supersymmetric contributions to the branching ratios for radiative flavor changing decays $\ell_i \rightarrow \ell_j \gamma$ relevant for muon and tau decays are then

$$\begin{aligned} \text{Br}(\ell_i \rightarrow \ell_j \gamma) &\simeq \frac{12\pi^3 \alpha (a_\mu^{\text{SUSY}})^2}{G_F^2 m_\mu^4} \left(|\epsilon_{Lij}|^2 + |\epsilon_{Rij}|^2 \right) \text{Br}(\ell_i \rightarrow \ell_j \bar{\nu}_{\ell_j} \nu_j) \\ &\simeq 1.85 \times 10^{14} (a_\mu^{\text{SUSY}})^2 \left(|\epsilon_{Lij}|^2 + |\epsilon_{Rij}|^2 \right) \text{Br}(\ell_i \rightarrow \ell_j \bar{\nu}_{\ell_j} \nu_j) \end{aligned} \quad (43)$$

where α is the fine structure constant, the muon weak decay rate is $\Gamma(\mu \rightarrow e \bar{\nu}_e \nu_\mu) = G_F^2 m_\mu^5 / (192\pi^3)$, $\text{Br}(\mu \rightarrow e \bar{\nu}_e \nu_\mu) \simeq 1$, and $\text{Br}(\tau \rightarrow \ell_j \bar{\nu}_{\ell_j} \nu_\tau) \simeq 0.175$. Note that the m_i dependence of the transition dipole coefficient (36) cancels with the m_i dependence of the radiative decay rate (35) within the branching ratio (43).

Left–left and right–right sflavor violating slepton mass squared mixings appear in the dimensionless flavor violating transition elements (41) and (42) in proportion to ratios of coupling constants, Bino to Wino masses which may be related to coupling constants under the assumption of gaugino unification $m_{\tilde{B}}/m_{\tilde{W}} = g_1^2/g_2^2$, and ratios and derivatives of loop functions. Since, as discussed above, the ratios and derivatives of loop functions do not depend drastically on the superpartner spectrum, left–left and right–right sflavor violating contributions to radiative flavor changing decays can then be related to the muon anomalous magnetic moment through the branching ratios (43) in a fairly model independent manner. In contrast left–right sflavor violating mass squared mixings appear in the transition elements (41) and (42) in proportion to slepton masses and $\tan \beta$. The relation between left–right mixings, the muon anomalous magnetic moment, and flavor changing branching ratios (43) is therefore model dependent. Therefore only the fairly model independent relations which can be extracted for left–left and right–right sflavor violating mass squared mixings are presented below.

If the current discrepancy [4] between a_μ^{exp} and a_μ^{SM} is interpreted as arising from supersymmetry, $a_\mu^{\text{SUSY}} \sim 43 \times 10^{-10}$, the current bound on $\mu \rightarrow e \gamma$ of $\text{Br}(\mu \rightarrow e \gamma) < 1.2 \times 10^{-11}$ [18] along with the relation (43) can be used to obtain a bound on the smuon–selectron transition dipole coefficients of

$$\sqrt{|\epsilon_{L21}|^2 + |\epsilon_{R21}|^2} \lesssim 6 \times 10^{-5}$$

In the absence of cancelations among the various contributions, this bound on the dipole coefficients may be used to bound the individual dimensionless sflavor violating mixings. Assuming a single contribution dominates then yields bounds on left–left and right–right selectron–smuon dimensionless mass squared mixing of

$$|(\delta_{12}^\ell)_{LL}| \lesssim 6 \times 10^{-5} (f'_{+,L})^{-1}$$

$$|(\delta_{12}^\ell)_{RR}| \lesssim 2 \times 10^{-3} \left(\frac{-f_0}{f_+} f'_{0,R} + \frac{h_0}{f_+} h'_{0,R} \right)^{-1}$$

where gaugino unification $m_{\tilde{B}}/m_{\tilde{W}} = g_1^2/g_2^2 = \tan^2 \theta$ has been assumed.

The bound obtained above on $(\delta_{12}^\ell)_{LL}$ is stronger by roughly a factor of 50–100 than a previously quoted bound [19]. The difference arises from a number of factors. In [19] only the chirality conserving photino diagram is considered, which is suppressed compared to the dominant chargino diagram by factors of gauge couplings, $\tan \beta$, and for equal superpartner masses, a smaller loop function. In addition there has also been an improvement in the experimental sensitivity to $\mu \rightarrow e\gamma$ radiative decays [18]. All these factors combine to provide a stronger constraint.

In analogy the the bounds derived above, the current bounds on flavor changing τ radiative decays of $\text{Br}(\tau \rightarrow \mu\gamma) < 1.1 \times 10^{-6}$ [20] and $\text{Br}(\tau \rightarrow e\gamma) < 2.7 \times 10^{-6}$ [21] along with the relation (43) can be used to obtain bounds on smuon–stau and selectron–stau dipole coefficients of

$$\sqrt{|\epsilon_{L32}|^2 + |\epsilon_{R32}|^2} \lesssim 4 \times 10^{-2}$$

$$\sqrt{|\epsilon_{L31}|^2 + |\epsilon_{R31}|^2} \lesssim 7 \times 10^{-2}$$

Assuming a single contribution dominates then yields the bounds on the left–left smuon–stau and selectron–stau dimensionless mass squared mixings of

$$|(\delta_{32}^\ell)_{LL}| \lesssim 4 \times 10^{-2} (f'_{+,L})^{-1}$$

$$|(\delta_{31}^\ell)_{LL}| \lesssim 7 \times 10^{-2} (f'_{+,L})^{-1}$$

where again gaugino unification has been assumed. Bounds on the right–right mixings are not significant since these insertions appear in subdominant diagrams

$$|(\delta_{32}^\ell)_{RR}| \lesssim 1.3 \left(\frac{-f_0}{f_+} f'_{0,R} + \frac{h_0}{f_+} h'_{0,R} \right)^{-1}$$

$$|(\delta_{31}^\ell)_{RR}| \lesssim 2.3 \left(\frac{-f_0}{f_+} f'_{0,R} + \frac{h_0}{f_+} h'_{0,R} \right)^{-1}$$

All the bounds given above are good for moderate to large $\tan\beta$ for which the first chargino diagram of Fig. 2 generally gives the dominant contribution. The only model dependence appears in the ratios and logarithmic derivatives of loop functions as indicated. If the current discrepancy [4] between a_μ^{exp} and a_μ^{SM} is interpreted as an upper limit on supersymmetric contributions, $a_\mu^{\text{SUSY}} \lesssim 43 \times 10^{-10}$, then the bounds given above may be interpreted as the most stringent possible bounds consistent with the muon anomalous magnetic moment.

5 Conclusions

Supersymmetry can give many interesting signals which may be observable in low energy processes. In this paper we have illuminated the relation between the muon anomalous magnetic moment, the electron EDM, and the lepton flavor violating radiative decays, $\mu \rightarrow e\gamma$, $\tau \rightarrow \mu\gamma$ and $\tau \rightarrow e\gamma$. A bound(measurement) of the non-Standard Model contributions to the muon anomalous magnetic moment can bound(determine) the overall scale of the dipole operators which contribute to these processes in a manner which is fairly insensitive to details of the superpartner mass spectrum. In this way the electron EDM and $\ell_i \rightarrow \ell_j\gamma$ decays can be related to small supersymmetric violations of time-reversal and slepton flavor respectively in a fairly model independent manner.

The Brookhaven muon $g-2$ experiment may eventually reach a sensitivity of $\Delta a_\mu^{\text{exp}} \sim 4 \times 10^{-10}$ [12]. If this sensitivity is achieved and the measured value is in agreement with an improved determination of the Standard Model

hadronic vacuum polarization and light by light scattering contributions then the bound on a_μ^{SUSY} would improve by approximately an order of magnitude. Such an agreement with the Standard Model would imply concomitantly heavier superpartners and weaken the bound given above on the phase of the dipole operator coming from the present ^{205}Tl EDM experiment [13] by an order of magnitude, and weaken the bounds given above on the slepton mixing amplitudes coming from the present $\ell_i \rightarrow \ell_j \gamma$ experiments [18, 20, 21] by a factor of roughly three. However, future EDM experiments in atomic traps may improve the sensitivity to the phase of the dipole operator by two to three orders of magnitude [22], and a future experiment sensitive to $\text{Br}(\mu \rightarrow e\gamma) \gtrsim 2 \times 10^{-14}$ [23] would improve the sensitivity to the selectron–smuon mixing amplitude by a factor of roughly 25.

The work of M.G. was supported by US Department of Energy. The work of S.T. was supported by the US National Science Foundation under grant PHY98-70115, the Alfred P. Sloan Foundation, and Stanford University through the Frederick E. Terman Fellowship.

A Supersymmetric Dipole Moments

Supersymmetric contributions to lepton electromagnetic dipole operators which couple to the up-type Higgs condensate are enhanced by a factor $\tan\beta$ with respect to couplings to the down-type Higgs condensate. As discussed in section 1 the contributions which are enhanced by this factor include a subset of the chirality violating diagrams of Fig. 2. In this appendix the expressions for these $\tan\beta$ enhanced contributions are presented. Gaugino–Higgsino mixing is treated perturbatively to first order as an insertion of a up-type Higgs condensate. Slepton proportionality is assumed in which the left-right mass squared mixing is given by $m_\ell \mu \tan\beta$ in the large $\tan\beta$ limit.

The supersymmetric contributions to \mathcal{D}_f may be expressed in terms of the dimensionless loop functions

$$J_N(x_1, x_2, \dots, x_N) \equiv \int_0^\infty dy y^2 \prod_{i=1}^N \frac{1}{y + x_i} \quad (44)$$

$$I_N(x_1, x_2, \dots, x_N) \equiv \int_0^\infty dy y \prod_{i=1}^N \frac{1}{y + x_i} \quad (45)$$

In terms of these functions, the chargino with sneutrino, Wino neutralino with left-handed slepton, Bino neutralino with left-handed slepton, Bino neutralino with right-handed slepton, and Bino neutralino with left-right mass squared insertion diagrams of Fig. 2 give, respectively,

$$\begin{aligned} \langle \tilde{W}^+ \tilde{H}_d^- \rangle : -2\mathcal{D}_f^{\chi^+} &= \frac{eg_2^2 \tan \beta}{32\pi^2} \frac{m_f}{\tilde{m}_H^4} \mu m_{\tilde{W}} \left(4J_5\left(\frac{m_{\tilde{\nu}_L}^2}{\tilde{m}_H^2}, \frac{\mu^2}{\tilde{m}_H^2}, \frac{m_{\tilde{W}}^2}{\tilde{m}_H^2}, \frac{\mu^2}{\tilde{m}_H^2}, \frac{\mu^2}{\tilde{m}_H^2}\right) \right. \\ &\quad + 4J_5\left(\frac{m_{\tilde{\nu}_L}^2}{\tilde{m}_H^2}, \frac{\mu^2}{\tilde{m}_H^2}, \frac{m_{\tilde{W}}^2}{\tilde{m}_H^2}, \frac{m_{\tilde{W}}^2}{\tilde{m}_H^2}, \frac{m_{\tilde{W}}^2}{\tilde{m}_H^2}\right) \\ &\quad \left. + 4J_5\left(\frac{m_{\tilde{\nu}_L}^2}{\tilde{m}_H^2}, \frac{\mu^2}{\tilde{m}_H^2}, \frac{m_{\tilde{W}}^2}{\tilde{m}_H^2}, \frac{m_{\tilde{W}}^2}{\tilde{m}_H^2}, \frac{\mu^2}{\tilde{m}_H^2}\right) \right) \\ &\equiv \frac{eg_2^2 \tan \beta}{32\pi^2} \frac{m_f}{\tilde{m}_H^4} \mu m_{\tilde{W}} f_+ \end{aligned} \quad (46)$$

$$\begin{aligned} \langle \tilde{W}^0 \tilde{H}_d^0 \rangle : -2\mathcal{D}_f^{\chi^0} &= -\frac{eg_2^2 \tan \beta}{192\pi^2} \frac{m_f}{\tilde{m}_H^4} \mu m_{\tilde{W}}^2 \left(12I_4\left(\frac{m_{\tilde{W}}^2}{\tilde{m}_H^2}, \frac{\mu^2}{\tilde{m}_H^2}, \frac{m_{\tilde{f}_L}^2}{\tilde{m}_H^2}, \frac{m_{\tilde{f}_L}^2}{\tilde{m}_H^2}\right) \right. \\ &\quad \left. - 12J_5\left(\frac{m_{\tilde{f}_L}^2}{\tilde{m}_H^2}, \frac{\mu^2}{\tilde{m}_H^2}, \frac{m_{\tilde{W}}^2}{\tilde{m}_H^2}, \frac{m_{\tilde{f}_L}^2}{\tilde{m}_H^2}, \frac{m_{\tilde{f}_L}^2}{\tilde{m}_H^2}\right) \right) \\ &\equiv -\frac{eg_2^2 \tan \beta}{192\pi^2} \frac{m_f}{\tilde{m}_H^4} \mu m_{\tilde{W}} f_{\tilde{W}^0 L} \end{aligned} \quad (47)$$

$$\begin{aligned} \langle \tilde{B} \tilde{H}_d \rangle : -2\mathcal{D}_f^{\chi^0 L} &= \frac{eg_1^2 \tan \beta}{192\pi^2} \frac{m_f}{\tilde{m}_H^4} \mu m_{\tilde{B}} \left(12I_4\left(\frac{m_{\tilde{B}}^2}{\tilde{m}_H^2}, \frac{\mu^2}{\tilde{m}_H^2}, \frac{m_{\tilde{f}_L}^2}{\tilde{m}_H^2}, \frac{m_{\tilde{f}_L}^2}{\tilde{m}_H^2}\right) \right. \\ &\quad \left. - 12J_5\left(\frac{m_{\tilde{f}_L}^2}{\tilde{m}_H^2}, \frac{\mu^2}{\tilde{m}_H^2}, \frac{m_{\tilde{B}}^2}{\tilde{m}_H^2}, \frac{m_{\tilde{f}_L}^2}{\tilde{m}_H^2}, \frac{m_{\tilde{f}_L}^2}{\tilde{m}_H^2}\right) \right) \\ &\equiv \frac{eg_1^2 \tan \beta}{192\pi^2} \frac{m_f}{\tilde{m}_H^4} \mu m_{\tilde{B}} f_{\tilde{B}L} \end{aligned} \quad (48)$$

$$\langle \tilde{B} \tilde{H}_d \rangle : -2\mathcal{D}_f^{\chi^0 R} = \frac{-2eg_1^2 \tan \beta}{192\pi^2} \frac{m_f}{\tilde{m}_H^4} \mu m_{\tilde{B}} \left(12I_4\left(\frac{m_{\tilde{B}}^2}{\tilde{m}_H^2}, \frac{\mu^2}{\tilde{m}_H^2}, \frac{m_{\tilde{f}_R}^2}{\tilde{m}_H^2}, \frac{m_{\tilde{f}_R}^2}{\tilde{m}_H^2}\right) \right)$$

$$-12J_5\left(\frac{m_{\tilde{f}_R}^2}{\tilde{m}_H^2}, \frac{\mu^2}{\tilde{m}_H^2}, \frac{m_{\tilde{B}}^2}{\tilde{m}_H^2}, \frac{m_{\tilde{f}_R}^2}{\tilde{m}_H^2}, \frac{m_{\tilde{f}_R}^2}{\tilde{m}_H^2}\right) \quad (49)$$

$$\equiv \frac{-2eg_1^2 \tan \beta}{192\pi^2} \frac{m_f}{\tilde{m}_H^4} \mu m_{\tilde{B}} f_{\tilde{B}R}$$

$$\langle \tilde{B}\tilde{B} \rangle : -2\mathcal{D}_f^{\chi_0 LR} = \frac{2eg_1^2 \tan \beta}{192\pi^2} \frac{m_f}{\tilde{m}_H^4} \mu m_{\tilde{B}} \left(6J_5\left(\frac{m_{\tilde{B}}^2}{\tilde{m}_H^2}, \frac{m_{\tilde{B}}^2}{\tilde{m}_H^2}, \frac{m_{\tilde{f}_L}^2}{\tilde{m}_H^2}, \frac{m_{\tilde{f}_R}^2}{\tilde{m}_H^2}, \frac{m_{\tilde{f}_R}^2}{\tilde{m}_H^2}\right) + 6J_5\left(\frac{m_{\tilde{B}}^2}{\tilde{m}_H^2}, \frac{m_{\tilde{B}}^2}{\tilde{m}_H^2}, \frac{m_{\tilde{f}_L}^2}{\tilde{m}_H^2}, \frac{m_{\tilde{f}_L}^2}{\tilde{m}_H^2}, \frac{m_{\tilde{f}_R}^2}{\tilde{m}_H^2}\right) \right) \quad (50)$$

$$\equiv \frac{2eg_1^2 \tan \beta}{192\pi^2} \frac{m_f}{\tilde{m}_H^4} \mu m_{\tilde{B}} h_0 . \quad (51)$$

In the text $f_{\tilde{B}R}$ is denoted by f_0 . The dependence of the loop functions f_i and h_0 on the mass ratios has been left implicit. The three neutralino diagrams of the first diagram in Fig. 1 are proportional to the same loop function evaluated with different arguments, as is evident from the above expressions. Also note that the factors in the large parentheses or, equivalently, the loop functions f_i and h_0 , are normalized to unity for equal superpartner masses. In particular, for equal superpartner masses $J_5(1, 1, 1, 1, 1) = 1/12$ and $I_4(1, 1, 1, 1) = 1/6$. Thus, for example, for such a spectrum the chargino diagram is $\propto (32\pi^2)^{-1}$. Note that a factor of \tilde{m}^{-4} has been factored out of the loop integrals in order to render them dimensionless; this may be any internal mass but for convenience it is chosen to the mass of the heaviest sparticle. The arbitrariness of this factoring follows from the scaling relations

$$J_N(x_1, \dots, x_N) = x_1^{3-N} J_N\left(1, \frac{x_2}{x_1}, \dots, \frac{x_N}{x_1}\right) \quad (52)$$

$$I_N(x_1, \dots, x_N) = x_1^{2-N} I_N\left(1, \frac{x_2}{x_1}, \dots, \frac{x_N}{x_1}\right) . \quad (53)$$

The contributions given above for the individual diagrams agree with those found in [6]. There appears to be a difference in the expressions for the chargino diagram and the first neutralino diagram of Fig. 2. This superficial difference is however a result of a different choice of routing the loop momenta. A numerical comparison between our results and those of [6] indicate no difference.

Analytic expressions may be obtained for the loop functions if only two mass scales appear.

$$J_5(x, 1, 1, 1, 1) = \frac{1}{6(x-1)^4} (1 - 6x + 3x^2 + 2x^3 - 6x^2 \ln x) , \quad (54)$$

$$\xrightarrow{x \ll 1} \frac{1}{6}(1 + O(x)) ,$$

$$J_5(x, x, 1, 1, 1) = \frac{1}{2(x-1)^4} (1 + 4x - 5x^2 + 2x(2+x) \ln x) , \quad (55)$$

$$\xrightarrow{x \ll 1} \frac{1}{2}(1 + O(x)) ,$$

$$J_5(x, x, x, 1, 1) = \frac{1}{2(x-1)^4} (-5 + 4x + x^2 - 2 \ln x - 4x \ln x) , \quad (56)$$

$$\xrightarrow{x \ll 1} \frac{1}{2}(-5 - 2 \ln x + O(x)) ,$$

$$J_5(x, x, x, x, 1) = \frac{1}{6(x-1)^4} \left(x^2 - 6x + 3 + \frac{2}{x} + 6 \ln x \right) , \quad (57)$$

$$\xrightarrow{x \ll 1} \frac{1}{6} \left(3 + \frac{2}{x} + 6 \ln x + O(x) \right) ,$$

$$I_4(x, 1, 1, 1) = \frac{1}{2(x-1)^3} (-1 + x^2 - 2x \ln x) , \quad (58)$$

$$\xrightarrow{x \ll 1} \frac{1}{2}(1 + O(x)) ,$$

$$I_4(x, x, 1, 1) = \frac{1}{2(x-1)^3} (2 - 2x + (1+x) \ln x) , \quad (59)$$

$$\xrightarrow{x \ll 1} -\frac{1}{2}(2 + \ln x) .$$

Note that $J_5(x, x, x, 1, 1) = x^{-2} J_5(x^{-1}, x^{-1}, 1, 1, 1)$ and $J_5(x, x, x, x, 1) = x^{-2} J_5(x^{-1}, 1, 1, 1, 1)$, which is an example of the more general relation in (52).

The loop functions appearing in the radiative transition dipole moments involve additional sflavor violating mass squared insertions beyond those of the flavor conserving dipole moments. The function

$$f'_{+,L} = \frac{m_{\nu L}^2}{f_+} \frac{\partial f_+}{\partial m_{\nu L}^2} = \frac{\partial \ln f_+}{\partial \ln m_{\nu L}^2} . \quad (60)$$

represents the sflavor insertion for the chargino–sneutrino diagram such that $f_+ f'_{+,L}$ is the loop function. The loop functions for the sflavor insertions for the three neutralino diagrams from the first neutralino diagram of Fig. 2 are described by the same loop function but with different arguments. These are represented by a subscript that indicates Bino or Wino coupling, and right-handed or left-handed sleptons

$$f'_{\tilde{B}L(R),L(R)} = \frac{m_{\tilde{\ell}_{L(R)}}^2}{f_{\tilde{B}L(R)}} \frac{\partial f_{\tilde{B}L(R)}}{\partial m_{\tilde{\ell}_{L(R)}}^2} = \frac{\partial \ln f_{\tilde{B}L(R)}}{\partial \ln m_{\tilde{\ell}_{L(R)}}^2},$$

$$f'_{\tilde{W}_0L,L} = \frac{m_{\tilde{\ell}_L}^2}{f_{\tilde{W}_0L}} \frac{\partial f_{\tilde{W}_0L}}{\partial m_{\tilde{\ell}_L}^2} = \frac{\partial \ln f_{\tilde{W}_0L}}{\partial \ln m_{\tilde{\ell}_L}^2}.$$

The sflavor violating mass squared insertions for the second neutralino diagram of Fig. 2 are represented by

$$h'_{0,L(R)} = \frac{m_{\tilde{\ell}_{L(R)}}^2}{h_0} \frac{\partial h_0}{\partial m_{\tilde{\ell}_{L(R)}}^2} = \frac{\partial \ln h_0}{\partial \ln m_{\tilde{\ell}_{L(R)}}^2},$$

$$h''_{0,LR} = \frac{m_{\tilde{\ell}_L}^2 m_{\tilde{\ell}_R}^2}{h_0} \frac{\partial^2 h_0}{\partial m_{\tilde{\ell}_L}^2 \partial m_{\tilde{\ell}_R}^2} = \frac{1}{h_0} \frac{\partial^2 h_0}{\partial \ln m_{\tilde{\ell}_L}^2 \partial \ln m_{\tilde{\ell}_R}^2}$$

such that $h_0 h'_{0,L(R)}$ and $h_0 h''_{0,LR}$ are the loop functions.

References

- [1] P. Fayet, in *Unification of the Fundamental Particle Interactions*, edited by S. Ferrara, J. Ellis, and P. van Nieuwenhuizen (Plenum, New York, 1980); J. A. Grifols and A. Mendez, Phys. Rev. **D26**, 1809 (1982); J. Ellis, J. Hagelin, D. V. Nanopoulos, Phys. Lett. **B116**, 283 (1982); R. Barbieri and L. Maiani, Phys. Lett. **B117**, 203 (1982).
- [2] J. Ellis, S. Ferrara, and D. Nanopoulos, Phys. Lett. B **114**, 231 (1982); W. Buchmuller and D. Wyler, Phys. Lett. B **121**, 321 (1983); F. del Aguila, M. Gavela, J. Grifols, and A. Mendez, Phys. Lett. B **126**, 71 (1983); J. Frere and M. Gavela, Phys. Lett. B **132**, 107 (1983); J.

- Polchinski and M. Wise, Phys. Lett. B **125**, 393 (1983); E. Franco and M. Mangano, Phys. Lett. B **135**, 445 (1984); J. Gerard, W. Grimus, A. Raychaudhuri, and G. Zoupanos, Phys. Lett. B **140**, 349 (1984); For a review of supersymmetric contributions to the electrom EDM see W. Bernreuther and M. Suzuki, Rev. Mod. Phys. **63**, 313 (1991); S. Abel, S. Khalil, and O. Lebedev, hep-ph/0103320.
- [3] M. Duncan, Nucl. Phys. B **221**, 285 (1983); J. Donoghue, J. Nilles, and D. Wyler, Phys. Lett. B **128**, 55 (1983).
- [4] H. N. Brown *et al.*, Muon $g - 2$ Collaboration, hep-ex/0102017, Phys. Rev. Lett. **86** 2227 (2001).
- [5] J. Hisano and Kazuhiro, hep-ph/0102315.
- [6] T. Moroi, hep-ph/9512396, Phys. Rev. D **53**, 6565 (1996) Erratum-ibid. D **56**, 4424 (1997).
- [7] M. Carena, G.F. Giudice and C.E.M. Wagner, hep-ph/9610233, Phys. Lett. B **390**, 234 (1997).
- [8] F. Borzumati, G. Farrar, N. Polonsky, S. Thomas, hep-ph/9902443, Nucl. Phys. B **555**, 53 (1999).
- [9] A. Czarnecki and W. Marciano, hep-ph/0102122.
- [10] W. Marciano and B. Roberts, hep-ph/0105056.
- [11] Lisa Everett, Gordon L. Kane, Stefano Rigolin, Lian-Tao Wang, hep-ph/0102145; Jonathan L. Feng and Konstantin T. Matchev, hep-ph/0102146; E.A. Baltz, P. Gondolo, hep-ph/0102147; Utpal Chattopadhyay, Pran Nath, hep-ph/0102157; R. Arnowitt, B. Dutta, Y. Santoso, hep-ph/0102181; Shinji Komine, Takeo Moroi, Masahiro Yamaguchi, hep-ph/0102204; T.W. Kephart and H. Pas, hep-ph/0102243; Tarek Ibrahim, Utpal Chattopadhyay, Pran Nath, hep-ph/0102324; J. Ellis, D.V. Nanopoulos, K.A. Olive, hep-ph/0102331; Kiwoon Choi, Kyuwan Hwang, Sin Kyu Kang, Kang Young Lee, and Wan Young

- Song, hep-ph/0103048; Stephen P. Martin and James D. Wells, hep-ph/0103067; S. Komine, T. Moroi, and M. Yamaguchi, hep-ph/0103182; K. Cheung, C.-H. Chou, and O. Kong, hep-ph/0103183; D.F. Carvalho, John Ellis, M.E. Gomez and S. Lola, hep-ph/0103256; H. Baer, C. Balazs, J. Ferrandis, and X. Tata, hep-ph/0103280; A. Bartl, T. Gajdosik, E. Lunghi, A. Masiero, W. Porod, H. Stremnitzer, and O. Vives, hep-ph/0103324.
- [12] R. Prigl, Muon $g - 2$ Collaboration, Proceedings of RADCOR2000, hep-ex/0101042.
- [13] E. Commins, S. Ross, D. DeMille, and B. Regan, Phys. Rev. A **50**, 2960 (1994).
- [14] S. Dimopoulos and S. Thomas, hep-ph/9510220, Nucl. Phys. B **465**, 23 (1996).
- [15] T. Ibrahim, P. Nath, hep-ph/9708456 Phys. Rev. D **57** 478 (1998), Erratum ibid. D **58** 019901 (1998), Erratum ibid. D **60** 079903 (1999), Erratum ibid. D **60** 119901 (1999); T. Ibrahim, P. Nath, hep-ph/9807501, Phys. Rev. D **58** 111301 (1998), Erratum ibid. D **60** 099902 (1999); M. Brhlik, G. Good, and G. Kane, hep-ph/9810457, Phys. Rev. D **59** 115004 (1999).
- [16] Some of the apparent accidental “cancellations” discussed in the literature are in fact not cancellations among physical phases, but arise simply from allowed field redefinitions by unphysical phases. Such misinterpretations of cancellations among phases may be avoided by working with basis independent combinations of physical phases.
- [17] Measurement of the final state lepton helicity, or angular distribution with polarized initial state, could distinguish the chiral structure of the transition dipole moment.
- [18] M. L. Brooks, *et al.*, MEGA Collaboration, hep-ex/9905013, Phys. Rev. Lett. **83**, 1521 (1999).

- [19] F. Gabbiani, E. Gabrielli, A. Masiero, and L. Silvestrini, Nucl. Phys. B **477**, 321 (1996).
- [20] S. Ahmed *et al.*, CLEO Collaboration, hep-ex/9910060, Phys. Rev. D **61**, 071101 (2000).
- [21] K. W. Edwards *et al.*, CLEO Collaboration, Phys. Rev. D **55**, 3919 (1997).
- [22] S. Chu, private communication.
- [23] T. Mori, *et al.*, <http://meg.psi.ch/doc/prop/index.html> (1999).